

## Supporting Information

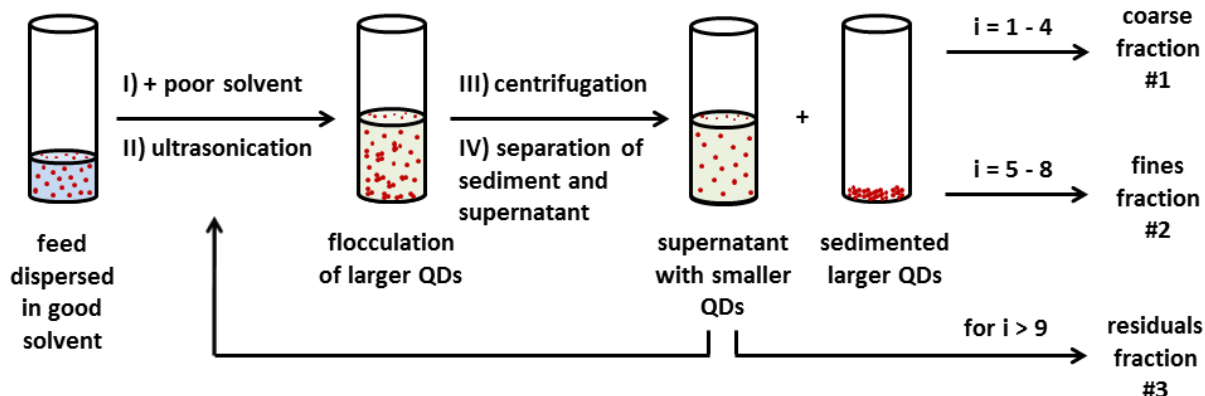
### Investigation of the size-property relationship in CuInS<sub>2</sub> quantum dots

Tugce Akdas<sup>1</sup>, Johannes Walter<sup>1</sup>, Doris Segets<sup>1</sup>, Monica Distaso<sup>1</sup>,  
Benjamin Winter<sup>2</sup>, Balaji Birajdar<sup>2</sup>, Erdmann Spiecker<sup>2</sup>, Wolfgang  
Peukert<sup>1,\*</sup>

<sup>1</sup> Institute of Particle Technology (LFG), Friedrich-Alexander-Universität Erlangen-Nürnberg (FAU), Cauerstr. 4, 91058 Erlangen, Germany

<sup>2</sup> Center for Nanoanalysis and Electron Microscopy (CENEM), Friedrich-Alexander-Universität Erlangen-Nürnberg (FAU), Cauerstr. 6, 91058 Erlangen, Germany

## 1. Scheme illustrating the size-selective precipitation (SSP) of the QDs:



**Scheme S1:** Illustration of the SSP procedure used for classifying  $\text{CuInS}_2$  QDs. Steps I-IV are repeated up to eight times (each cycle= $i$ ), leading to the coarse ( $i=1-4$ ), fines ( $i=5-8$ ) and residuals fractions ( $i>9$ ). The residuals fraction is obtained by evaporating the supernatant.

**Table S1:** Overview of three exemplary experiments and the masses of each obtained fraction.

| sample  |      | experiment 1 | experiment 2 | experiment 3 | mean values     |
|---------|------|--------------|--------------|--------------|-----------------|
| feed    | [mg] | 268.3        | 278.3        | 276.4        | $274.3 \pm 5.3$ |
|         | [%]  | 100.0        | 100.0        | 100.0        | $100.0 \pm 0.0$ |
| #1      | [mg] | 241.3        | 247.3        | 252.8        | $247.1 \pm 5.8$ |
|         | [%]  | 89.9         | 88.9         | 91.5         | $90.1 \pm 1.3$  |
| #2      | [mg] | 15.9         | 9.9          | 6.1          | $10.6 \pm 4.9$  |
|         | [%]  | 5.9          | 3.6          | 2.2          | $3.9 \pm 1.9$   |
| #3      | [mg] | 8.5          | 5.8          | 5.5          | $6.6 \pm 1.7$   |
|         | [%]  | 3.2          | 2.1          | 2.0          | $2.4 \pm 0.7$   |
| missing | [mg] | 2.6          | 15.3         | 12.0         | $10.0 \pm 6.6$  |
|         | [%]  | 1.0          | 5.5          | 4.3          | $3.6 \pm 2.3$   |

The reproducibility of the experiments was checked by performing the same experiments from various batches. In Table S1 three representative experiments are given exemplarily. A high purity and cleanliness is necessary for successful SSP. As the amount of material was relatively low for fractions #2 and #3, the characterization of these fractions via XRD and TGA could only be repeated once.

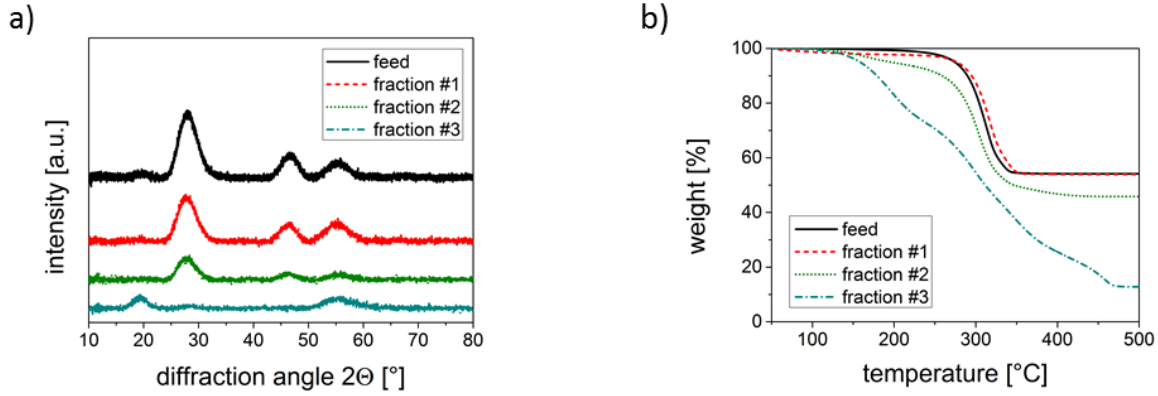


**Figure S1:** a) X-ray diffraction pattern of the feed (black line), coarse fraction #1 (red line), fines fraction #2 (green line) and residuals fraction #3 (cyan blue line). b) Gives the results of TG analysis of the feed (black line), coarse fraction #1 (red dashed line), fines fraction #2 (green dotted line) and residuals fraction #3 (cyan blue dashed-dotted line).

## 2. Theoretical background of analytical ultracentrifugation (AUC):

The Lamm equation provides a thermodynamic approach of the centrifugation process by considering the movement of particles due to sedimentation and diffusion in a mass conservation approach<sup>1</sup>:

$$\frac{\partial c}{\partial t} = \underbrace{D \left( \frac{\partial^2 c}{\partial r^2} + \frac{1}{r} \frac{\partial c}{\partial r} \right)}_{\text{diffusion}} - \underbrace{\omega^2 s \left( r \frac{\partial c}{\partial r} + 2c \right)}_{\text{sedimentation}} \quad (S1)$$

$\partial c / \partial t$  is the change in mass concentration with time as a function of the radius  $r$ . The sedimentation coefficient  $s$  has the dimension of time and is usually expressed in Svedberg with 1 sved equal  $10^{-13}$  seconds. The Svedberg equation correlates the sedimentation and the diffusion coefficient:

$$M = \frac{sRT}{D(1 - \bar{v}\rho_s)} \quad (S2)$$

$M$  denotes the molar mass of the particle,  $R$  is the gas constant,  $T$  is the temperature of the experiment in Kelvin,  $\rho_s$  is the density of the solvent and  $\bar{v}$  is the partial specific volume, which is the inverse of the particle density. With known particle density and solvent parameters the hydrodynamic diameter of the particles can be calculated according to Stokes' equation:

$$x_h = \sqrt{\frac{18\eta s}{\rho_p - \rho_s}} \quad (S3)$$

$\eta$  is the viscosity of the solvent and  $\rho_s$  is the density of the particle. Using the direct boundary  $c(s)$  model implemented in Sedfit, the sedimentation coefficients

distribution can be determined. The  $c(s)$  model calculates the distribution of the diffusion corrected sedimentation coefficients by fitting the experimental data to the direct solution of the Lamm equation<sup>2</sup>. However, it assumes a spherical particle shape and a constant  $\bar{v}$  for the 1-dimensional parameterization. In contrast, the  $c(s,D)$  model also allows for variations in the partial specific volume for particles of known shape by spanning a 2-dimensional grid of  $s$  and  $D$  values<sup>3</sup>. For spherical particles the partial specific volume and size of the particles can be calculated without prior knowledge on the QDs by using the sedimentation and diffusion coefficient distributions<sup>4-5</sup>.

Herein, it has to be noted that the resolution of the 2-dimensional  $c(s,D)$  model in Sedfit is limited by the maximum number of grid points, which can be computed (900 points in our case). The software Ultrascan3 offers a much higher resolution as it can access supercomputing capabilities in combination with the 2-dimensional spectrum analysis (2DSA)<sup>6</sup>. However, the current 2DSA model does not include regularization, which would be required to stabilize the solution of Lamm's equation. Thus, evaluation of polydisperse samples such as considered in this work is not possible so far because heavy peak splitting is observed during analysis using 2DSA.

### **3. Results of 2-dimensional AUC analysis:**

For the feed, coarse fraction #1 and residuals fraction #3 one main species is obtained each, whereas two species were found for the fines fraction #2. Further, it becomes clear that the distributions of the feed and fraction #1 are very similar with a comparably narrow range of sedimentation coefficients. In contrast, fraction #2 reveals a second main species at 6.96 sved, which was not observable in the feed before. For fraction #3, a much faster sedimenting species with a very broad sedimentation coefficient distribution is found.

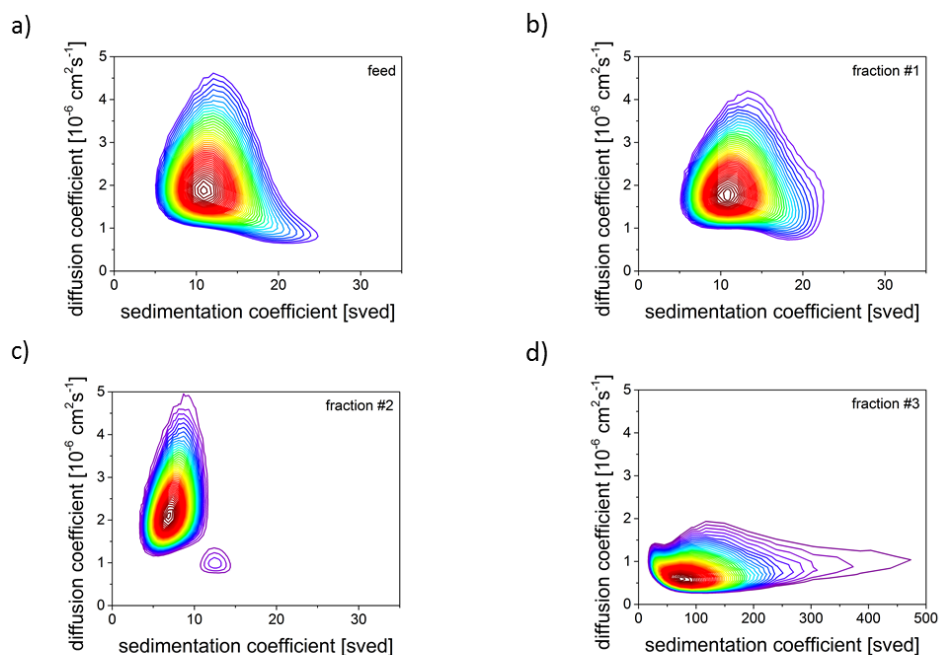


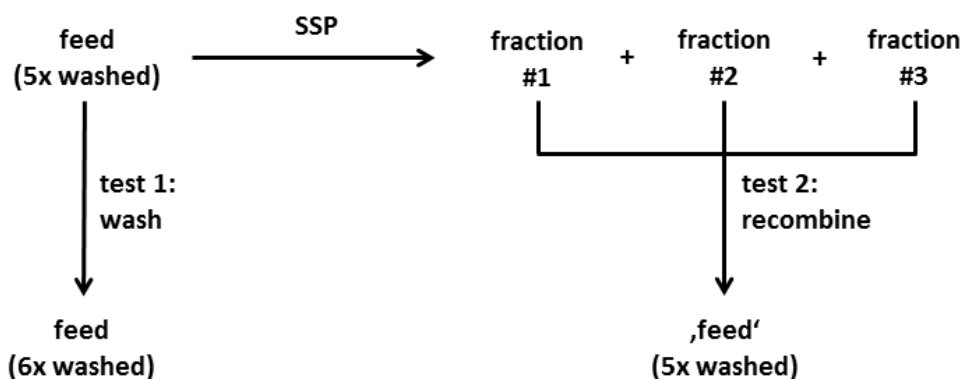
**Figure S2:** 2-dimensional sedimentation and diffusion coefficient distributions of the a) feed, b) coarse fraction #1, c) fines fraction #2 and d) residuals fraction #3 as obtained by the  $c(s,D)$  analysis performed using Sedfit, Version 14.6e. Colours from purple to red indicate a higher relative concentration.

#### 4. Summary of the optical data:

**Table S2:** Summary of the data derived from optical analysis of the feed sample, the coarse fraction #1, the fines fraction #2 and the residuals fraction #3. The values were obtained from three separate experiments with standard deviations as indicated.

| sample      | absorption maxima |                 | emission maxima |                 | FWHM            | PL QY         |
|-------------|-------------------|-----------------|-----------------|-----------------|-----------------|---------------|
|             | Abs 1 [nm]        | Abs 2 [nm]      | Emi 1 [nm]      | Emi 2 [nm]      | [nm]            | [%]           |
| feed        | $475.7 \pm 1.2$   | $548.8 \pm 2.9$ | $640.1 \pm 0.3$ | $663.1 \pm 2.8$ | $105.7 \pm 0.3$ | $0.8 \pm 0.1$ |
| fraction #1 | $475.0 \pm 2.0$   | $548.8 \pm 2.9$ | $639.8 \pm 0.8$ | $662.9 \pm 3.5$ | $105.4 \pm 0.7$ | $1.0 \pm 0.1$ |
| fraction #2 | $473.0 \pm 1.7$   | -               | $622.6 \pm 2.7$ | -               | $91.3 \pm 1.6$  | $0.5 \pm 0.1$ |
| fraction #3 | $473.5 \pm 2.1$   | -               | $624.7 \pm 0.4$ | -               | $94.4 \pm 0.8$  | $0.2 \pm 0.1$ |

## 5. Additional experiments:



Scheme S2: Illustration of the tests to check the origin of the emission behavior after SSP.

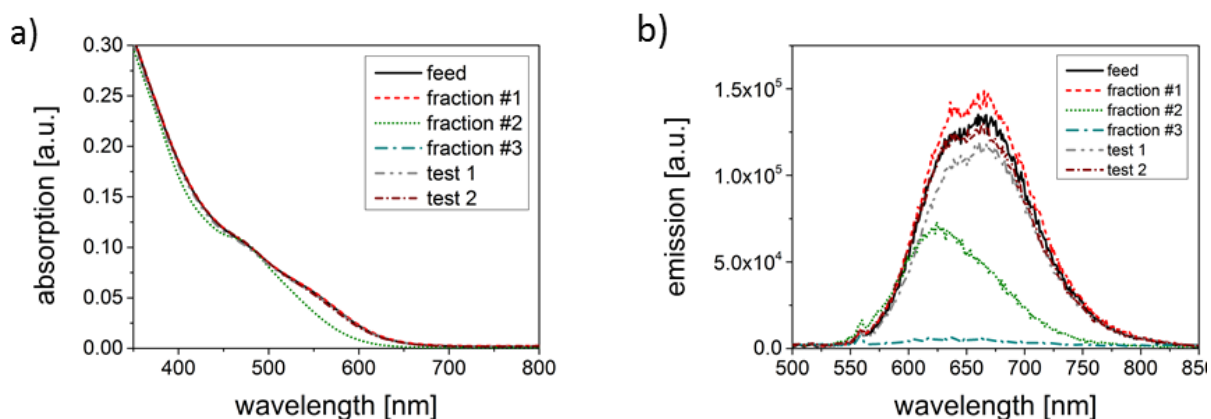


**Figure S3:** Photoluminescence spectra of the feed (black solid line), the coarse fraction #1 (red dashed line), the fines fraction #2 (green dotted line) and the residuals fraction #3 (cyan blue dashed-dotted line) and the spectra of the samples on which additional tests were performed, namely additional washing of the feed (test 1, grey dashed-dotted-dotted line) and the back mixed fractions (test 2, brown dashed-dotted-dashed line). All samples were diluted to an optical density of 0.1 at 480 nm, the excitation wavelength was  $\lambda_{\text{exc}} = 480$  nm.

### Remarks to test 1:

In previous work<sup>7</sup> we had reported that the emission intensity of non-stoichiometric CuInS<sub>2</sub> QDs depends on the purification and thus on the organic surrounding of the nanocrystals. The more effective the purification, i.e. the less organics in the sample, the lower is the emission intensity. The results shown here on stoichiometric CuInS<sub>2</sub> QDs hint in the same direction: When comparing the emission spectrum of the feed washed five times with the emission spectrum of the feed washed six times (test 1, Figure S3b), it becomes evident that with increasing number of purification cycles, the emission of the sample as a whole is decreasing. This is in accordance with reports on other material systems<sup>8</sup>.

**Remarks to test 2:**

As the supernatant after SSP is not thrown away but kept as fraction #3, the whole initial sample consisting of particles and organics is retained. Thus, recombination of all fractions back to one single sample results in a sample that seems to be identical to the feed at first glance. Nevertheless, it has to be considered that this sample was in contact with antisolvents and changes will have occurred on the molecular level quite certainly: (i) a certain fraction of organic molecules might not be attached to the surface anymore as strongly as prior to the SSP procedure and (ii) a certain mass loss has occurred which might not be just due to particle losses but also due to organic losses.

These two reasons might explain the fact that the emission intensity of the 'feed' sample after recombination does not have exactly the same emission over the entire wavelength range as before. However, the absorption spectrum seems to be less prone to such small changes – in accordance with the fact that the missing smaller particles of fraction #2 are not recognized in the absorption spectrum of fraction #1.

**Table S3: Summary of the size-dependent  $\Delta E_{\text{gap}}$  values from calibration vs. AUC data.**

| <b>Size (nm)</b> | <b><math>\Delta E_{\text{gap}}</math> (eV)</b> |
|------------------|--|
| 2.8              | 2.04   |
| 3.0              | 1.99   |
| 3.2              | 1.94   |
| 3.4              | 1.91   |
| 3.6              | 1.87   |
| 3.8              | 1.85   |
| 4.0              | 1.82   |
| 4.2              | 1.80   |
| 4.4              | 1.78   |
| 4.6              | 1.77   |
| 4.8              | 1.75   |
| 5.0              | 1.74   |
| 5.2              | 1.73   |
| 5.4              | 1.72   |
| 5.6              | 1.71   |
| 5.8              | 1.70   |
| 6.0              | 1.69   |
| 6.2              | 1.68   |
| 6.4              | 1.67   |
| 6.6              | 1.67   |
| 6.8              | 1.66   |
| 7.0              | 1.65   |
| 7.2              | 1.65   |
| 7.4              | 1.64   |
| 7.6              | 1.64   |
| 7.8              | 1.63   |
| 8.0              | 1.63   |
| 8.2              | 1.63   |
| 8.4              | 1.62   |
| 8.6              | 1.62   |
| 8.8              | 1.62   |
| 9.0              | 1.61   |
| 9.2              | 1.61   |
| 9.4              | 1.61   |
| 9.6              | 1.61   |
| 9.8              | 1.60   |
| 10.0             | 1.60   |

## References

1. Schuck, P., Size-distribution analysis of macromolecules by sedimentation velocity ultracentrifugation and Lamm equation modeling. *Biophysical Journal* **2000**, 78 (3), 1606-1619.
2. Schuck, P., Sedimentation analysis of noninteracting and self-associating solutes using numerical solutions to the Lamm equation. *Biophysical Journal* **1998**, 75 (3), 1503-1512.
3. Brown, P. H.; Schuck, P., Macromolecular size-and-shape distributions by sedimentation velocity analytical ultracentrifugation. *Biophysical Journal* **2006**, 90 (12), 4651-4661.
4. Carney, R. P.; Kim, J. Y.; Qian, H.; Jin, R.; Mehenni, H.; Stellacci, F.; Bakr, O. M., Determination of nanoparticle size distribution together with density or molecular weight by 2D analytical ultracentrifugation. *Nature Communications* **2011**, 2.
5. Demeler, B.; Tich-Lam, N.; Gorbet, G. E.; Schirf, V.; Brookes, E. H.; Mulvaney, P.; El-Ballouli, A. a. O.; Pan, J.; Bakr, O. M.; Demeler, A. K.; Uribe, B. I. H.; Bhattarai, N.; Whetten, R. L., Characterization of Size, Anisotropy, and Density Heterogeneity of Nanoparticles by Sedimentation Velocity. *Analytical Chemistry* **2014**, 86 (15), 7688-7695.
6. Brookes, E.; Cao, W.; Demeler, B., A Two-Dimensional Spectrum Analysis for Sedimentation Velocity Experiments of Mixtures with Heterogeneity in Molecular Weight and Shape. *Eur. Biophys. J.* **2010**, 39 (3), 405-14.
7. Akdas, T.; Distaso, M.; Kuhri, S.; Winter, B.; Birajdar, B.; Spiecker, E.; Guldi, D. M.; Peukert, W., The effects of post-processing on the surface and the optical properties of copper indium sulfide quantum dots. *Journal of Colloid and Interface Science* **2015**, 445, 337-347.
8. Kalyuzhny, G.; Murray, R. W., Ligand effects on optical properties of CdSe nanocrystals. *Journal of Physical Chemistry B* **2005**, 109 (15), 7012-7021.